# Transformer protection based on the increment of flux linkages

**Article** *in* IEE Proceedings - Generation Transmission and Distribution · August 2004

DOI: 10.1049/ip-gtd:20040378 · Source: IEEE Xplore



**4 authors**, including:

Y.C. Kang
Chonbuk National University
**190** PUBLICATIONS **3,273** CITATIONS
SEE PROFILE

P.A. Crossley
Manchester Power Solutions
**277** PUBLICATIONS **7,095** CITATIONS
SEE PROFILE

Study Committee B5 Colloquium
2005 September 14-16
Calgary, CANADA

108

# TRANSFORMER PROTECTION RELAY BASED ON THE INCREMENT OF THE FLUX LINKAGES

**Y. C. Kang*** **B.E. Lee** **S.H. Kang** **Y.G. Kim** **I.D. Kim** **P.A. Crossley**

**Chonbuk Nat'l Univ.** **Myongji Univ.** **Hankook IED** **Doowon Col.** **Queen's Univ. of Belfast (UK)**

**NPTC (Korea)**

The ratio of the increments of the primary and secondary winding flux linkages (RIFL) is the same as the turns ratio during normal operating conditions such as magnetic inrush, over-excitation and external faults. For an internal fault, the RIFL is not equal to the turns ratio. This paper proposes a transformer protection relay using the RIFL. For a single-phase or a three-phase Y-Y transformer, the increments of the flux linkages are calculated. For a three-phase Y-Δ transformer, the differences between the two phases of the increments of the flux linkages are calculated to use the line currents, because the delta winding current is unavailable. The RIFL is compared against the turns ratio; if they are different, it is an internal fault. The performance of the proposed relay was compared with the conventional current differential relay with harmonic blocking. Test results indicate that the proposed relay successfully discriminates between internal winding faults and magnetic inrush and reduces the operating time of the relay for internal faults. This paper also describes the results of implementation of the algorithm into a digital signal processor based prototype relay.

Keywords: Magnetizing Inrush, Remanent Flux, Increments of the Flux Linkages

## 1. NOMENCLATURE

| Symbols | Definition |
|---|---|
| $v_1$, $v_2$ | Voltages |
| $i_1$, $i_2$ | Currents |
| $\lambda_1$, $\lambda_2$ | Flux linkages |
| $R_1$, $R_2$ | Winding resistances |
| $L_{l1}$, $L_{l2}$ | Leakage inductances |
| $\phi_m$ | Mutual flux |
| $N_1$, $N_2$ | Number of turns |
| $v_A$, $v_B$, $v_C$ | Primary voltages (3ϕ) |
| $i_A$, $i_B$, $i_C$ | Primary currents (3ϕ) |
| $i_a$, $i_b$, $i_c$ | Secondary line currents (3ϕ) |
| $R_A$, $R_B$, $R_C$ | Primary winding resistances (3ϕ) |
| $L_{lA}$, $L_{lB}$, $L_{lC}$ | Primary leakage inductances (3ϕ) |
| $\lambda_A$, $\lambda_B$, $\lambda_C$ | Primary flux linkages (3ϕ) |

yckang@chonbuk.ac.kr

| | |
|---|---|
| $v_{ab}$, $v_{bc}$, $v_{ca}$ | Secondary voltages (3ϕ) |
| $i_{ab}$, $i_{bc}$, $i_{ca}$ | Secondary winding currents (3ϕ) |
| $R_{ab}$, $R_{bc}$, $R_{ca}$ | Secondary winding resistances (3ϕ) |
| $L_{lab}$, $L_{lbc}$, $L_{lca}$ | Secondary leakage inductances (3ϕ) |
| $\lambda_{ab}$, $\lambda_{bc}$, $\lambda_{ca}$ | Secondary flux linkages (3ϕ) |

## 2. INTRODUCTION

Current differential relays are widely used to detect internal faults in power transformers. To prevent mal-operation during magnetic inrush or over-excitation, these relays adopt three kinds of restraints, i.e. current, voltage, and flux.

For current derived restraints, second- and fifth-harmonic components are used [1–3]. Harmonic restraints ensure stability during transformer energisation and over-excitation, but may reduce the operating sensitivity on internal faults. Moreover, problems are experienced if the harmonic content in the operating current is low.

A flux-restrained current differential relay was proposed in [4]. As difficulty arises in obtaining the initial core flux, the restraining signal is based on not flux but the derivative of the flux over the differential current. However, it is valid only when the primary current equals the magnetizing current i.e. the load is not connected. In addition, it used the winding current, which is unavailable in a three-phase transformer including a delta winding.

Techniques have been reported that do not depend on the harmonic characteristic of the differential current, but rely on the electro-magnetic differential equations [5, 6]. These require voltage and current signals and consequently can only be used when voltage signals are available.

The algorithm in [5] uses the linear elements and thus does not rely on the core condition. It detects internal faults by checking whether the three differential equations, derived from the primary and secondary windings, are valid. For a single-phase and a wye-wye transformer, the fault can be detected directly by checking the three equations since the winding currents are available. On the contrary, for a wye-delta transformer, each of the three equations contains the delta winding currents, which are practically unavailable. To use the line current, the algorithm decomposed the winding current into circulating and non-circulating currents. The latter could be estimated from the line currents while the former could not be obtained analytically. Thus, each equation still has four terms containing the circulating components and they cannot be obtained analytically. The fault detection procedure for a wye-delta transformer is composed as follows. The ‘Reference Phase’ out of three phases is first chosen. Secondly, the four terms for the ‘Reference Phase’ are calculated using the remainder of the equation. Thirdly, they are substituted into the other equations for the other two phases after being multiplied by factors; these include the parameters of the ‘Reference Phase’ and the other phases. Finally, the algorithm detects an internal fault if the multiplied and substituted terms do not satisfy any other equations. The procedure assumes the X/R ratios of the delta winding are large. The faulted phase can be identified based on the results when all the three phases are used as the ‘Reference Phase’ [8]. In addition, for a delta-delta transformer, each equation has eight terms containing the circulating currents, because primary and secondary windings have their winding currents. Thus, the conversion factors that should contain the parameters of the Reference and the other phases of both windings, will be in a more complicated form.

The basic principle of transformer protection using the ratio of the induced voltages of the primary and secondary windings was proposed in [6]. The internal fault is detected based on comparing induced voltages or induced voltage differences with turns ratio. It approximates the differential terms using the backward Euler method and may cause some errors if it is implemented in a digital relay. This paper describes a transformer protective relaying algorithm that uses the ratio of the increment of the primary and secondary winding flux linkages (RIFL). It is the integral version of the algorithm in [6]. For magnetic inrush and over-excitation, the RIFL is equal to the turns ratio, while for an internal fault, it is not. The algorithm estimates the increments of flux linkages for a single phase and a three-phase wye-wye transformer. On the contrary, for a wye-delta transformer, it estimates the differences of the increments of the flux linkages between the two phases to use the line currents. Then, the matching increments or differences of the increments are compared with the turns ratio. The performance of the proposed relay was tested and compared with the conventional current differential relay with harmonic blocking for magnetic inrush and internal faults. The paper also describes the results of implementation of the algorithm on a digital signal processor based prototype relay.

## 3. TRANSFORMER PROTECTION RELAY USING THE RATIO OF FLUX LINKAGES

### *3.1 A single-phase transformer*

Fig. 1 shows a two winding single-phase transformer. If there is no internal fault, $v_1$ and $v_2$ can be given by:

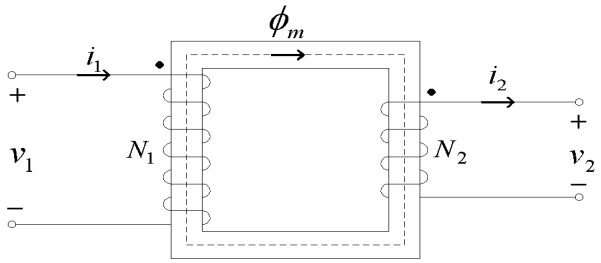


Fig. 1 A two winding single-phase transformer

$$v_1 = R_1 i_1 + L_{l1}\frac{di_1}{dt} + \frac{d\lambda_1}{dt} \tag{1}$$

$$v_2 = -R_2 i_2 - L_{l2}\frac{di_2}{dt} + \frac{d\lambda_2}{dt} \tag{2}$$

Rearranging (1) and (2) yields:

$$\frac{d\lambda_1}{dt} = v_1 - R_1 i_1 - L_{l1}\frac{di_1}{dt} \tag{3}$$

$$\frac{d\lambda_2}{dt} = v_2 + R_2 i_2 + L_{l2}\frac{di_2}{dt} \tag{4}$$

The increments of the flux linkages, $\Delta\lambda_1$, $\Delta\lambda_2$, are estimated by integrating (3) and (4). The ratio of the increment of the primary and secondary winding flux linkages (RIFL) is then defined as:

$$RIFL \equiv \frac{\Delta\lambda_1}{\Delta\lambda_2} \tag{5}$$

In the steady state, the RIFL is the same as the turns ratio ($N_1/N_2$) except when $\Delta\lambda_1 = 0$ or $\Delta\lambda_2 = 0$. For magnetic inrush and overexcitation, the RIFL is also equal to $N_1/N_2$, although $\Delta\lambda_1$ and $\Delta\lambda_2$ are non-sinusoidal and distorted. For internal faults, the RIFL is not the same as $N_1/N_2$.

From this point, the RIFL can be directly used for discriminating internal faults from magnetizing inrush and overexcitation. However even for normal operating conditions, the RIFL is not always equal to $N_1/N_2$ because $\Delta\lambda_1$ and $\Delta\lambda_2$ are instantaneous values and consequently pass through zero. In order to overcome the problem, the Detector described by (6) is used to detect a fault in this paper. The Detector measures the percentage difference between the two estimated increments of the flux linkages. If (6) is less than a threshold, the transformer is not faulted; if greater, it is.

$$Detector = \frac{\Delta\lambda_1 - \frac{N_1}{N_2}\Delta\lambda_2}{\sqrt{2}V_1 \cdot T} \times 100\ (\%) \tag{6}$$

where, $T$ is the sampling interval

### *3.2 A three-phase Y-Δ transformer*

Fig. 2 shows the connections of a three-phase Y-Δ transformer. Voltages are represented in (7)–(12).

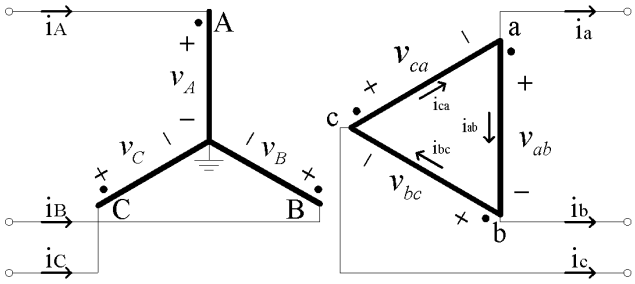


Fig. 2 A two winding three-phase wye-delta transformer

$$v_A = R_A i_A + L_{lA}\frac{di_A}{dt} + \frac{d\lambda_A}{dt} \tag{7}$$

$$v_B = R_B i_B + L_{lB}\frac{di_B}{dt} + \frac{d\lambda_B}{dt} \tag{8}$$

$$v_C = R_C i_C + L_{lC}\frac{di_C}{dt} + \frac{d\lambda_C}{dt} \tag{9}$$

$$v_{ab} = R_{ab} i_{ab} + L_{lab}\frac{di_{ab}}{dt} + \frac{d\lambda_{ab}}{dt} \tag{10}$$

$$v_{bc} = R_{bc} i_{bc} + L_{lbc}\frac{di_{bc}}{dt} + \frac{d\lambda_{bc}}{dt} \tag{11}$$

$$v_{ca} = R_{ca} i_{ca} + L_{lca}\frac{di_{ca}}{dt} + \frac{d\lambda_{ca}}{dt} \tag{12}$$

If there is no internal fault, (13) is valid.

$$\frac{\Delta\lambda_A}{\Delta\lambda_{ab}} = \frac{N_1}{N_2},\ \frac{\Delta\lambda_B}{\Delta\lambda_{bc}} = \frac{N_1}{N_2},\ \frac{\Delta\lambda_C}{\Delta\lambda_{ca}} = \frac{N_1}{N_2} \tag{13}$$

If $\Delta\lambda_A$, $\Delta\lambda_B$, $\Delta\lambda_C$, $\Delta\lambda_{ab}$, $\Delta\lambda_{bc}$, and $\Delta\lambda_{ca}$ can be calculated from (7)–(12), the three Detectors can be derived directly from (13). $\Delta\lambda_A$, $\Delta\lambda_B$, $\Delta\lambda_C$, can be calculated, but $\Delta\lambda_{ab}$, $\Delta\lambda_{bc}$, and $\Delta\lambda_{ca}$ cannot from (10)–(12) because $i_{ab}$, $i_{bc}$, and $i_{ca}$ are unavailable. In [5], $i_{ab}$, $i_{bc}$ and $i_{ca}$ were decomposed into the non-circulating and circulating currents. The non-circulating current could be derived from the line current. However, the terms relating the circulating currents could not be obtained analytically and thus an alternative was used to detect an internal fault as mentioned in Introduction.

In this paper, to use the line currents, the following relationship between the line and winding currents on the secondary winding is used.

$$i_{ca} - i_{ab} = i_a,\ i_{ab} - i_{bc} = i_b,\ i_{bc} - i_{ca} = i_c \tag{14}$$

In addition, if there is no internal fault, the assumption in (15) is valid.

$$R_{ab} \approx R_{bc} \approx R_{ca} = R,\ L_{lab} \approx L_{lbc} \approx L_{lca} = L_l \tag{15}$$

Subtracting (10) from (12), (11) from (10) and (12) from (11) yields:

$$\frac{d\lambda_{ca}}{dt} - \frac{d\lambda_{ab}}{dt} = v_{ca} - v_{ab} - Ri_a - L_l\frac{di_a}{dt} \tag{16}$$

$$\frac{d\lambda_{ab}}{dt} - \frac{d\lambda_{bc}}{dt} = v_{ab} - v_{bc} - Ri_b - L_l\frac{di_b}{dt} \tag{17}$$

$$\frac{d\lambda_{bc}}{dt} - \frac{d\lambda_{ca}}{dt} = v_{bc} - v_{ca} - Ri_c - L_l \frac{di_c}{dt} \tag{18}$$

Therefore, whilst $\Delta\lambda_{ab}$, $\Delta\lambda_{bc}$, and $\Delta\lambda_{ca}$ cannot be calculated, their differences between the two phases can be calculated by integrating (16)–(18). The corresponding equations to (16), (17) and (18) can be derived from (7)–(9):

$$\frac{d\lambda_C}{dt} - \frac{d\lambda_A}{dt} = v_C - v_A - (R_C i_C - R_A i_A) - \left( L_{lC} \frac{di_C}{dt} - L_{lA} \frac{di_A}{dt} \right) \tag{19}$$

$$\frac{d\lambda_A}{dt} - \frac{d\lambda_B}{dt} = v_A - v_B - (R_A i_A - R_B i_B) - \left( L_{lA} \frac{di_A}{dt} - L_{lB} \frac{di_B}{dt} \right) \tag{20}$$

$$\frac{d\lambda_B}{dt} - \frac{d\lambda_C}{dt} = v_B - v_C - (R_B i_B - R_C i_C) - \left( L_{lB} \frac{di_B}{dt} - L_{lC} \frac{di_C}{dt} \right) \tag{21}$$

On the other hand, the relationship between the differences of the increments of the flux linkages can be derived by:

$$\frac{\Delta\lambda_C - \Delta\lambda_A}{\Delta\lambda_{ca} - \Delta\lambda_{ab}} = \frac{N_1}{N_2}, \frac{\Delta\lambda_A - \Delta\lambda_B}{\Delta\lambda_{ab} - \Delta\lambda_{bc}} = \frac{N_1}{N_2}, \frac{\Delta\lambda_B - \Delta\lambda_C}{\Delta\lambda_{bc} - \Delta\lambda_{ca}} = \frac{N_1}{N_2} \tag{22}$$

Equation (22) is a necessary and sufficient condition for (13). Its proof is shown in Appendix. In this paper, (22) is used for fault detection for a Y-Δ transformer.

Thus, the three Detectors are given by:

$$Detector\ 1 = \frac{\Delta(\lambda_C - \lambda_A) - \frac{N_1}{N_2}\Delta(\lambda_{ca} - \lambda_{ab})}{\sqrt{2}V_{CA} \cdot T} \times 100\ (\%) \tag{23}$$

$$Detector\ 2 = \frac{\Delta(\lambda_A - \lambda_B) - \frac{N_1}{N_2}\Delta(\lambda_{ab} - \lambda_{bc})}{\sqrt{2}V_{AB} \cdot T} \times 100\ (\%) \tag{24}$$

$$Detector\ 3 = \frac{\Delta(\lambda_B - \lambda_C) - \frac{N_1}{N_2}\Delta(\lambda_{bc} - \lambda_{ca})}{\sqrt{2}V_{BC} \cdot T} \times 100\ (\%) \tag{25}$$

## 4. CASE STUDIES

Fig. 3 shows a single-diagram of the simulated system and the power frequency is 60 Hz. A two-winding three-phase Y-Δ transformer (154kV/12.7kV, 55 MVA) is used to generate fault and inrush data using EMTP. The hysteresis characteristics of the transformer core are modeled using a type-96 element; the saturation point of (40 A, 334 Vs) is selected to use HYSDAT, a subroutine of EMTP. The internal winding fault modeling techniques in [7] are used to represent turn-to-ground and turn-to-turn faults.

The sampling rate is 32 samples/cycle (s/c) and the voltages and currents are passed through the Butterworth 2nd order filters with a stop-band cut-off frequency of 960 Hz (half the sampling frequency).

The conventional relay with harmonic blocking was compared with the proposed relay. The characteristic of the relay is:

$$I_d > K_1 I_r + I_{offset} \tag{26}$$

where, $K_1 = 0.3$, $I_{offset} = 15\ A$

For the second harmonic Blocking, (27) is used.

$$I_d < K_2 I_{d2} \tag{27}$$

where, $K_2 = 10$ was used in this paper.

The performance of the proposed algorithm was verified on the various conditions such as magnetic inrush and internal winding faults.

### *4.1 Magnetic inrush*

The magnitude of the inrush current depends on the energisation angle, the remanent flux at the instant of energisation and load. Thus, different inrush currents are generated by varying the above parameters and used for test.

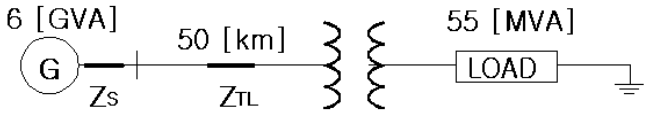


Fig. 3 Model system studied

*Case 1: energisation angle of 0 deg, 80% remanent flux, no load*

Figs. 4–6 show the results for Case 1. The transformer was energized at 50.1 ms. The current and voltages are severely distorted as shown in Fig. 4. Fig. 5 shows the two components of Detector 1 i.e. $\Delta(\lambda_C - \lambda_A)$ and $N_1/N_2\Delta(\lambda_{ca} - \lambda_{ab})$. The results show that the two estimated differences of the increments of the flux linkages are nearly the same even if the currents and voltages are distorted.

If the Detector output is greater than 5%, a counter is increased by one; otherwise it is decreased by one. If the counter is less than zero, it is reset to zero. If a counter exceeds four, the final trip signal is issued. Fig. 6 shows the three Detectors and the trip signal. The output of from each of the three Detectors are less than 5%, consequently the trip signal is not activated.

Fig. 7 shows the operating response of the conventional current differential relay with harmonic blocking. The 87 relay was issued at 3.5 ms after energisation. As expected, the blocking signal is issued 0.4 ms after energisation since the ratio of $I_{d2}/I_d$ exceeds the threshold and maintained during magnetic inrush. Thus the trip signal was not activated.

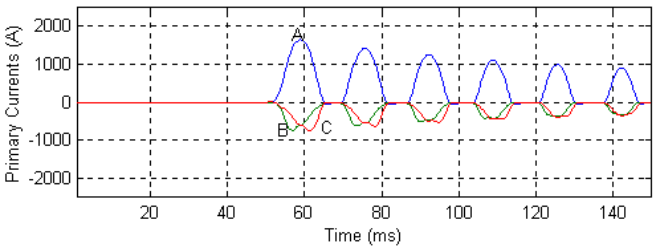


(a) Primary currents

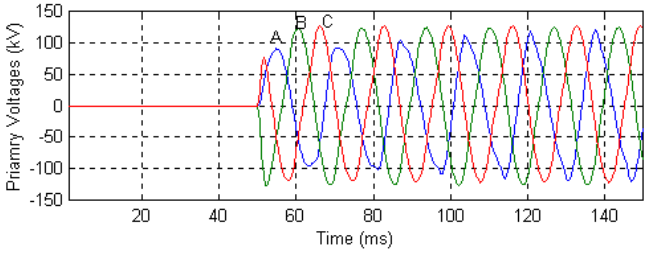


(b) Primary voltages ($v_A$, $v_B$, $v_C$)

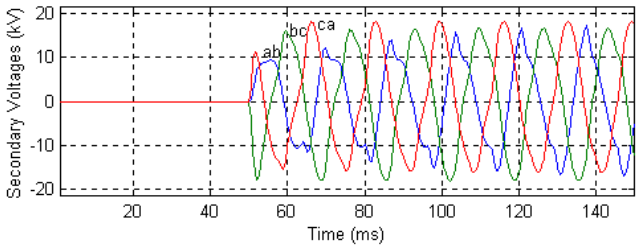


(c) Secondary voltages ($v_{ab}$, $v_{bc}$, $v_{ca}$)

Fig. 4 Three-phase currents and voltages

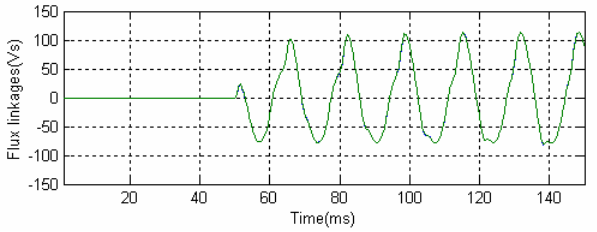


(a) $\Delta(\lambda_C - \lambda_A)$ and $N_1/N_2\Delta(\lambda_{ca} - \lambda_{ab})$ of Detector 1

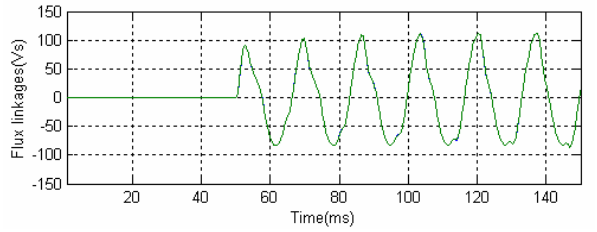


(b) $\Delta(\lambda_A - \lambda_B)$ and $N_1/N_2\Delta(\lambda_{ab} - \lambda_{bc})$of Detector 2

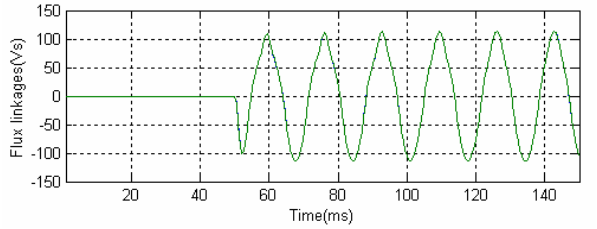


(c) $\Delta(\lambda_B - \lambda_C)$ and $N_1/N_2\Delta(\lambda_{bc} - \lambda_{ca})$ of Detector 3

Fig. 5 Differences of the estimated increments of the flux linkages

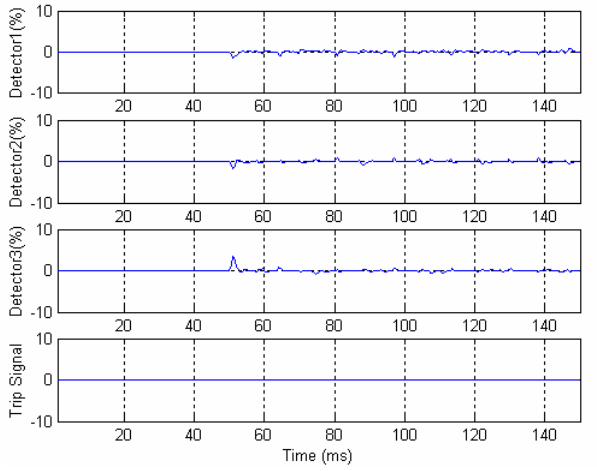


Fig. 6 Detectors and the trip signal for Case 1

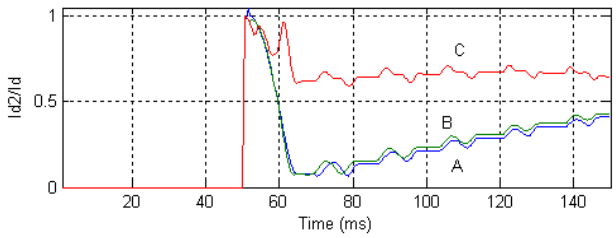


(a) Ratio of $I_{d2}/I_d$

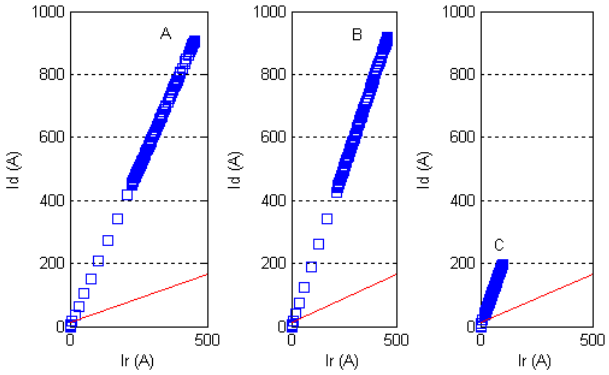


(b) Operating response of the conventional relay

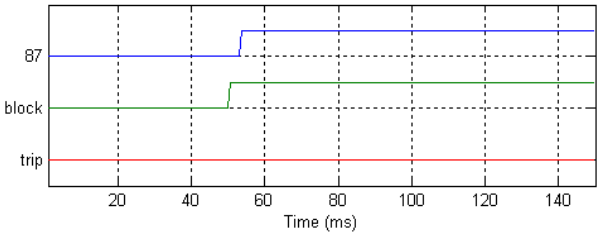


(c) 87, blocking and trip signals

Fig. 7 Results for the conventional relay for Case 1

*Case 2: energisation angle of 0 deg, 80 % remanent flux, full load*

Fig. 8 shows the operating response of the three Detectors for Case 2; this is identical to Case 1, except a full load (55 MVA) is connected to the transformer secondary. The primary and secondary voltages are also severely distorted. All three detectors remain below 5%, consequently the trip signal is not activated.

The two results indicate that the relay accurately estimates the differences of the increments of the flux linkages, even though the currents and voltages are severely distorted by the high remanent flux and the load current.

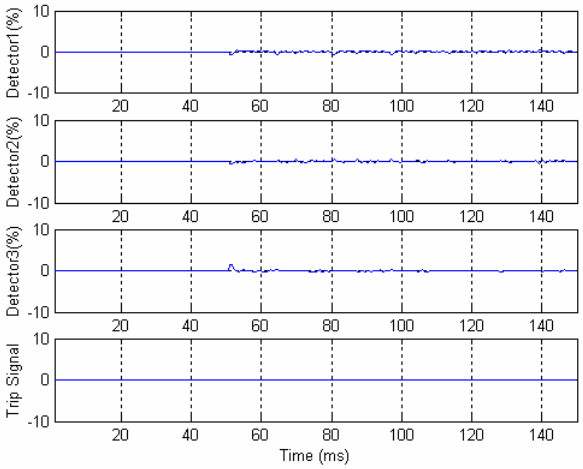


Fig. 8 Detectors and the trip signal for Case 2

## *4.2 Internal winding faults*

The fault data for various faults on the phase B of primary winding are generated and used to test the algorithm. The test results for two of the fault scenarios are described in Case 3.

*Case 3: A turn-to-ground fault, located 60 % from the neutral winding end and at 0 deg inception angle.*

Fig. 9 shows the operating response of the three Detectors for Case 3. The fault occurred at 39.0 ms. As the differences of the increments of the flux linkages are not the same and thus Detectors 2 and 3 exceed the 5%

operating threshold. The signals in Detector 1 remain small, because it not affected by a fault on phase B. In Case 3, the trip signal is activated 2.7 ms after fault occurrence.

Fig. 10 shows the results of the conventional relay for Case 2. '87' was issued at 7.4 ms after fault occurrence. The blocking signal was issued at 39.6 ms after fault occurrence and maintained for 12 ms. The trip signal is activated at 13.1 ms after fault occurrence. Thus the proposed relay was 10.4 ms faster than the conventional relay.

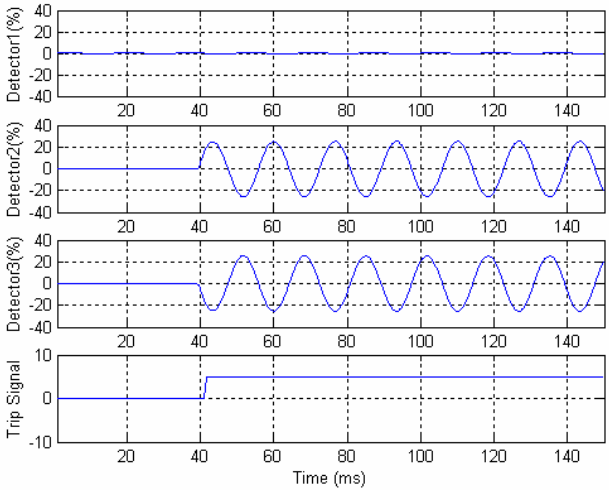


Fig. 9 Detectors and the trip signal for Case 3

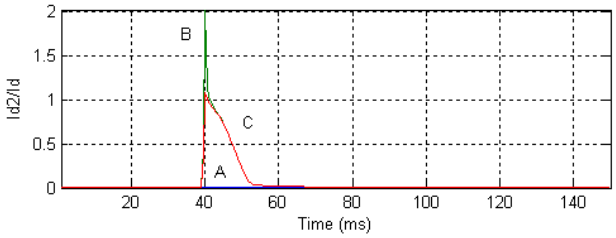


(a) Ratio of $I_{d2}/I_d$

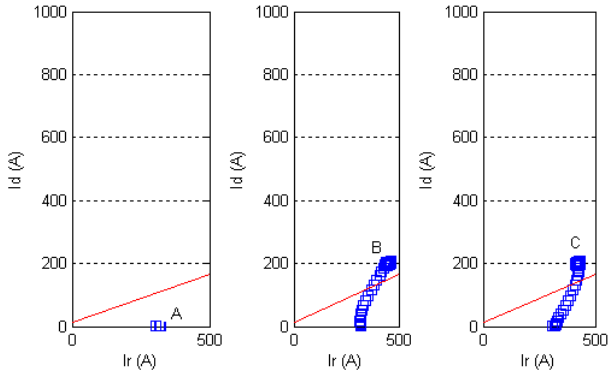


(b) Operating responses of the conventional relay

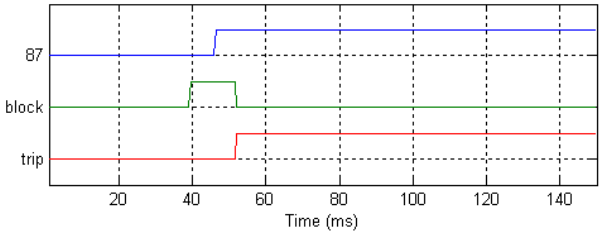


(c) 87, blocking and trip signals

Fig. 10 Results for the conventional relay for Case 3

## 5. HARDWARE IMPLEMENTATION

Fig. 11 shows the configuration of the prototype system. The relay was implemented on the TMS320C6701

digital signal processor. The sampling rate is 32 s/c. The currents and voltages are passed through Butterworth 2nd order filters ($f_c$ = 960 Hz), which are Sallen & Key active filters, to the 14-bit A/D converter.

Figs. 12 and 13 show the results for Case 1. Noise signals in the hardware result in the larger errors than observed in the simulation results. However, the algorithm performs well with the same threshold value of 5% and security counter of 4.

Fig. 14 shows the results for Case 3. The trip signal is activated 2.6 ms after fault occurrence. Consequently, the prototype relay can successfully discriminate between internal faults and magnetic inrush.

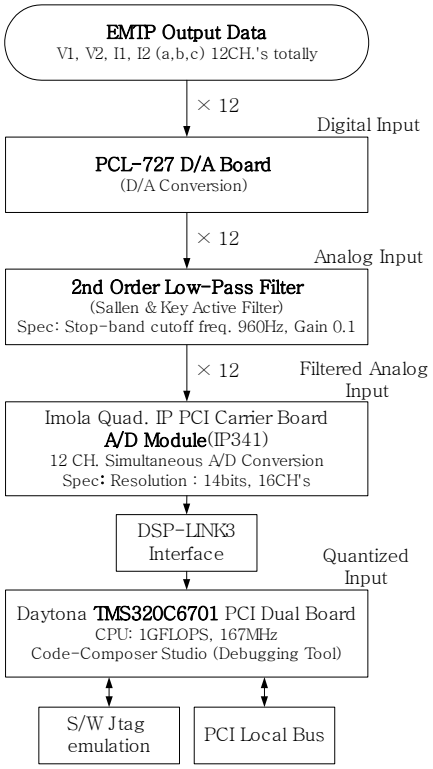


Fig. 11 Configuration of hardware implementation

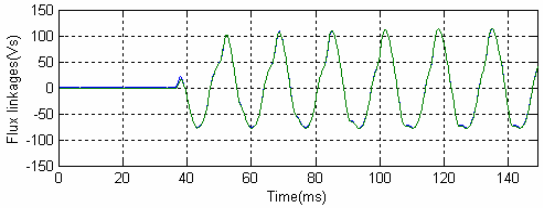


(a) $\Delta(\lambda_C - \lambda_A)$ and $N_1/N_2\Delta(\lambda_{ca} - \lambda_{ab})$ of Detector 1

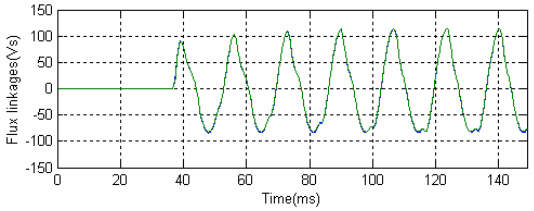


(b) $\Delta(\lambda_A - \lambda_B)$ and $N_1/N_2\Delta(\lambda_{ab} - \lambda_{bc})$of Detector 2

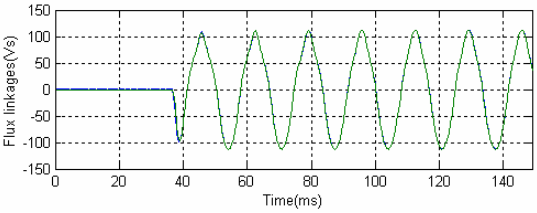


(c) $\Delta(\lambda_B - \lambda_C)$ and $N_1/N_2\Delta(\lambda_{bc} - \lambda_{ca})$ of Detector 3

Fig. 12 Estimated induced voltage differences for Case 1

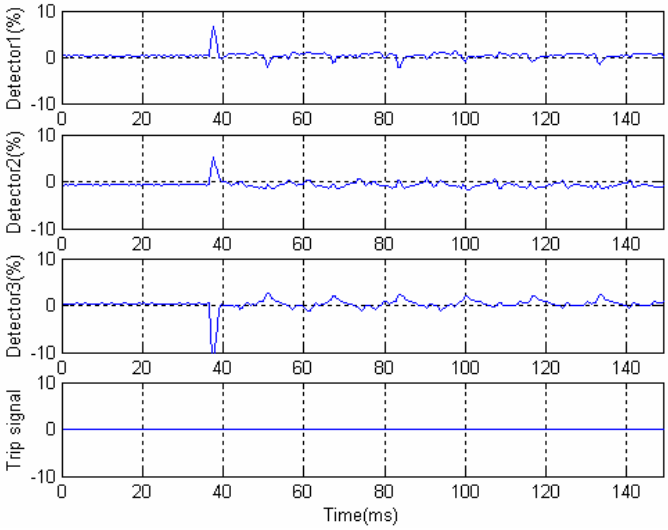

Fig. 13 The results of hardware implementation for Case 1

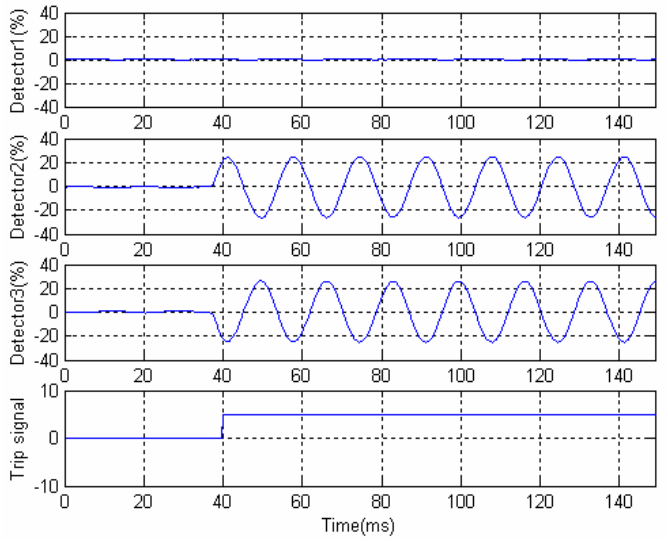

Fig. 14 The results of hardware implementation for Case 3

## 6. CONCLUSION

This paper describes a transformer protection relay based on the ratio of the increment of the primary and secondary flux linkages. The relay estimates the increments of the flux linkages for a wye-wye transformer or the differences of the increments of the flux linkages for a transformer including a delta winding to use the line currents instead of the winding currents. It compares them with the turns ratio to discriminate internal faults from magnetic inrush.

The test results clearly demonstrate that the proposed algorithm remains stable for magnetic inrush. In addition, the relay detects internal faults within a fraction of one cycle. The operating time was reduced by about 10 ms compared with the conventional relay with harmonic blocking. A prototype relay successfully discriminates between internal faults and magnetic inrush.

The algorithm does not need to know the hysteresis characteristics of the transformer core and the use of time domain signals ensures the operating time is less than a conventional relay.

## 7. ACKNOWLEDGEMENTS

This work was sponsored by Korea Ministry of Science and Technology and Korea Science and Engineering Foundation through the ERC program (Next-Generation Power Technology Center, NPTC).

## 8. REFERENCES


[1] C. D. Hayward, "Harmonic-Current-Restrained Relays for Transformer Differential Protection," [AIEE Trans. vol. 60, pp. 377–382, 1941]

[2] R. L. Sharp, W. E. Glassburn, "A Transformer Differential Relay with Second-Harmonic Restraint," [AIEE Trans. Part III, vol. 77, pp. 913–918, 1958]

[3] C. H. Einvall, J. R. Linders, "A Three-phase Differential Relay for Transformer Protection," [IEEE Trans. on PAS, vol. 94, no. 6, pp. 1971–1980, November/December 1975]

[4] A. G. Phadke, J. S. Thorp, "A New Computer-Based Flux-Restrained Current-Differential Relay for Power Transformer Protection," [IEEE Trans. on PAS, vol.102, no. 11, pp. 3624–3629, November 1983]

[5] M. S. Sachdev, T. S. Sidhu, H.C. Wood, "A Digital Relaying Algorithm for Detecting Transformer Winding Faults," [IEEE Trans. on PWRD, vol. 4, no. 3, pp. 1638–1648, July 1989]

[6] Y. C. Kang, B. E. Lee, S. H. Kang, S. S. Kim, J.K. Lee, "A Transformer Protective Relaying Algorithm Using the Ratio of Induced Voltages," [IEEE PES 2001 SM, July 15–19, 2001, Vancouver, BC, Canada]

[7] P. Bastard, P. Bertrand, M. Meunier, "A Transformer Model for Winding Fault Studies," [IEEE Trans. on PWRD, vol. 9, no. 2, pp. 690–699, April 1994]